Applied Thermal Engineering 217 (2022) 119272

Contents lists available at ScienceDirect

Applied Thermal Engineering

journal homepage: www.elsevier.com/locate/apthermeng

Thermal enhancement of rectangular channels using hook-shaped fins and dimples

Omar Khaled [a], John Swift [b], Roger Kempers [a,*]

[a] Department of Mechanical Engineering, York University, Toronto, Canada
[b] NUCAP Energy, 3370 Pharmacy Avenue, Toronto, Canada

ARTICLE INFO

Keywords:
Forced convection
Convection enhancement
GRIPMetal
Fins
Air cooling
Skiving

ABSTRACT

A common technique for enhancing convective heat transfer from a surface is to add extended surfaces (fins); the size and shape of these fins play a crucial role in their performance. Many studies have investigated ways to leverage novel manufacturing techniques to create different fin shapes to improve thermal-fluidic performance. A skiving process which creates a unique array of hook-shaped raised features (hooks) and cavities (dimples) on metal surfaces (GRIPMetal) has been developed. The present work experimentally characterizes the thermal and hydraulic performance of rectangular channels with an array of these hooks and dimples on their opposing major surfaces and compares these channels to channels with bare surfaces and other fin structures. Three different hook sizes with nominal hook heights, h, of 1 mm, 1.5 mm and 2.25 mm and different inter-fin spacings were investigated. The effect of tip clearance above the hooks, C, was investigated for clearances of h, 2 h, 4 h, 6.5 h. Results were obtained for air at Reynolds numbers from 4,000 to 20,000. The overall Nusselt numbers and friction factors were calculated, and empirical correlations were developed through nonlinear multivariable regression. The array of hooks increased the Nusselt number, Nu_h, up to a factor of 4 depending on Re, while the maximum increase in the friction factor, f_h, was 12 at the highest Re. Generally, increasing the tip clearance decreased the friction factor and Nusselt number for the channel. Hook height and inter-fin spacings have no effect on thermal performance at high tip clearances (above $C = 4\ h$), while the hydraulic performance shows a recognizable dependency.

1. Introduction

The rapid advances in a wide variety of engineering applications, such as heat exchangers, gas turbine blades, telecommunications, aerospace and electronics devices require effective and reliable surface cooling techniques. Pin fins added to the flow field have been used as a potential technique to enhance heat transfer from surfaces [1–4]. Pin fins can be classified into short and long fins, with short fins classified as having pin-height-to-diameter ratios, h/D, of between 0.5 and 4, while long fins have h/D of more than 4. Despite short fins' heat transfer being typically lower than that of long fins [5–8] short pin fins are commonly used for cooling applications in compact spaces such as gas turbines, cooling of electronic devices, and aerospace applications [9].

The addition of pin fins enhances the heat transfer of surfaces in two ways: First, they increase the heat transfer surface area. Second, they produce horseshoe vortices on the upstream endwall (uncovered fin region) of the pin fin and wake vortices downstream which subsequently generate high turbulence and mixing [10]. For short fins, the additional area contribution to heat transfer improvement is relatively low and the turbulent mixing component is the more dominant factor. In contrast to long fins arrays where heat transfer from endwalls is relatively negligible, the short fins arrays exhibit endwall heat transfer that is comparable to the heat transfer from the fins themselves [5,11,12]. The heat transfer from these endwalls depends strongly on the geometry of the pin fins and their distribution [13]. Consequently, the correlations that represent the heat transfer and the pressure drop for the long fins are not suitable for the short fins [5].

In the last few decades, heat transfer and pressure drop performance of the flow over arrays of short pin fins to better understand their flow characteristics have been the subject of extensive investigation. For instance, Sparrow et al. [14] showed that a staggered arrangement of fins generally has better heat transfer capabilities and a greater pressure drop penalty than in-line arrays; this difference increases as the pin-height-to-diameter ratio, h/D, increases. Lawson et al. [15] and Ferster et al. [16] demonstrated that heat transfer augmentation depends more

* Corresponding author.
E-mail address: kempers@yorku.ca (R. Kempers).

https://doi.org/10.1016/j.applthermaleng.2022.119272
Received 15 December 2021; Received in revised form 31 May 2022; Accepted 2 September 2022
Available online 7 September 2022
1359-4311/© 2022 Elsevier Ltd. All rights reserved.

Nomenclature

A_b	Base area subjected to the heat flux (m^2)
C_h	Clearance between two adjacent rows of hooks (mm)
C	Tip clearance (m)
C_d	Drag coefficient of an array of hooks
C_p	Specific heat capacity of air at the average bulk temperature (J/kgK)
D_h	Hydraulic diameter (m)
f_{Dh}	Friction factor based on the hydraulic diameter
f_h	Friction factor based on the hook height
f_o	Friction factor of flat plate
h_{lm}	Convective heat transfer coefficient based on logarithmic mean temperature (W/m^2K)
h_{bulk}	Convective heat transfer coefficient based on average temperature difference (W/m^2K)
h	Hook height (mm)
H	Test section channel height (m)
h_{lm}	Heat transfer coefficient (W/m^2K)
h_{bulk}	Heat transfer coefficient (W/m^2K)
k	Thermal conductivity of air at the average bulk temperature (W/mK)
L_f	Length of the test section (m)
L_c	Characteristic length (m)
L_h	Hook length (mm)
L_g	Groove length (mm)
Nu_{Dh}	Nusselt number based on the hydraulic diameter
Nu_h	Nusselt number based on hook height
Nu_o	Nusselt number of flat plate
ΔP	Pressure drop across the heat sink (Pa)
Pr	Prandtl number of air at the average bulk temperature
Q_{loss}	Heat loss rate (W)
Q_{elec}	Electrical input power (W)
R_{loss}	Heat loss resistance (K/W)
Re_a	Reynolds number based on the array velocity
Re	Reynolds number based on inlet velocity
Re^*	Modified Reynolds number for rectangular channels
S_T	Spanwise spacing (mm)
S_L	Streamwise spacing (mm)
ΔT_{lm}	Logarithmic mean temperature difference (K)
ΔT_{bulk}	Average temperature difference between the surface and the air (K)
T_i	Fluid inlet bulk temperature (°C)
T_o	Fluid outlet bulk temperature (°C)
$T_{s,avg}$	Test section average surface temperature (°C)
$T_{s,i}$	Test section inlet surface temperature (°C)
$T_{s,o}$	Test section outlet surface temperature (°C)
T_{amb}	Ambient temperature (°C)
V_a	Array velocity (m/s)
V_{in}	Mean inlet velocity (m/s)
W_h	Hook width (mm)
W	Test section channel width (mm)
ρ	Density of the of air at the average bulk temperature (kg/m^3)
μ	Dynamic viscosity of air at the average bulk temperature (Pas)
η	Thermal performance factor

on the streamwise spacing than the spanwise spacing, while the opposite is true for pressure drop. They also concluded that to increase heat transfer with the lowest pressure drop penalty, streamwise spacings should be minimized and spanwise spacing should be maximized. This was consistent with the findings of Lyall et al. [17] which indicate that increasing the spanwise spacing decreases the pressure drop for a single row array.

Sparrow and Kadle [18] were the first to investigate the effect of introducing a tip clearance on the heat transfer of a longitudinal fin array. They concluded that for clearance-to-fin-height ratios of 0.1, 0.2 and 0.3, the heat transfer decreased by 85 %, 74 %, and 64 %, respectively, when compared with the no-clearance case. Garimella and Eibeck [19] tested the effect of tip clearance-to-fin-height ratio on the heat transfer and pressure drop characteristics of rectangular pin fins. Their results show that heat transfer decreases with increasing tip clearance and becomes independent of *Re* at high values of *C/h*. Jubran et al. [20] experimentally investigated the effects of inter-fin spacing and tip clearance on the heat transfer from in-line and staggered circular pin fin arrays. They discovered that a staggered array has a greater heat transfer rate, regardless of the value of the tip clearance, and increasing the tip clearance to equal the fin height results in a 40 % reduction in heat transfer compared with the no-clearance case. Moores and Joshi [21] examined the effect of tip clearance for a liquid-cooled array of circular pins fins. They concluded that low tip clearance values enhance heat transfer due to the additional heat transfer area added from the tips.

Tip clearances also generate three-dimensional vortices at the tips that promote mixing, thereby enhancing heat transfer. More recently, Tabkhi et al. [22] experimentally and numerically showed that the presence of tip clearance significantly enhances heat transfer in the wake region through improving the three dimensionality of the vortices downstream of the fin and shortening the wake region.

Much effort has also gone into exploring the cross-sectional shapes of pin fins to optimize the performance of these arrays beyond those of circular pins. Metzger et al. [23] experimentally compared the heat transfer and pressure drop characteristics of circular and oblong pin fins with varying angles of attack and showed that the heat transfer of oblong pin fins is higher than that of the circular pins by a maximum of 20 % but at the expense of having double the pressure drop. Similarly, Chyu et al. [24] studied an array of cubic/diamond fins using the naphthalene sublimation technique and heat/mass transfer analogy. They found that heat transfer for the cubic pin fins is 40 % and 80 % higher than that of the diamond and the circular arrays, respectively. Sahiti et al. [25] numerically investigated the influence of several pin fin cross sections (NACA airfoil, drop shape, lancet, elliptic, circular, and square) on the heat transfer performance for both staggered and in-line arrays. Their results show that either the elliptic or the drop-form pin fins are superior to the others depending on the geometrical parameters of the array (pin length, transverse and longitudinal spacings, and coverage ratio). Also, the heat transfer and pressure drop of six different pin fin cross sections (circular, elliptic, oblong, drop-form, NACA, and lancet) in a staggered array were compared experimentally by Xi et al. [26]. They concluded that the circular pin fin had the largest heat transfer but also had the maximum pressure drop penalty when compared with other shapes. The elliptical pin fins showed a superior thermal performance to the others because of their very low pressure drop with a moderate heat transfer.

Another method of enhancing heat transfer from pin fin arrays is the introduction of dimples in the array. Chyu et al. [27] experimentally compared the heat transfer performance from a dimpled rectangular channel and a smooth flat plate. The dimples were circular, and teardrop shaped. Both shapes showed higher heat transfer than that of the smooth plate by a factor of 2.5. The effect of changing dimple shapes on the heat transfer and pressure drop was also experimentally and numerically investigated by Rao et al [28]. Their results show that heat transfer enhancement is greatly influenced by dimple shape. For instance, the enhancement for a teardrop-shaped dimple ranged from 1.89 to 2, depending on the *Re* when compared with a smooth flat plate. This

enhancement is 18 % greater than that of conventional spherical dimples and 28 % greater than that of elliptical ones. On the other hand, the pressure drop did not exhibit any dependency on the shape except for the teardrop-shaped dimple for which the friction factor was 1.6–2.3 times the smooth flat plate friction factor. Moon et al. [29] studied the heat transfer and pressure drop of array characteristics of circular dimples at different channel heights. Their results show that heat transfer augmentation due to these dimples with respect to a smooth flat plate is approximately constant by a factor of 2.1. In addition, both pressure drop and heat transfer are independent of channel height. More recently, Gao et al. [30] experimentally studied both the liquid and vapor flow of R134a over a dimpled flat plate in a rectangular channel. The comparison between the obtained results and a correlation for a flat plate with the same aspect ratio showed that the presence of dimples resulted in multiplying both the friction factor and the Nusselt number by a factor of up to 15.7 and 8.6, respectively. Rao et al. [31] introduced the concept of hybrid pin fin–dimple arrays. They experimentally compared the thermal and hydraulic performance of pin fin–dimple and pin fin arrays and dimple depth on performance. They showed that the presence of dimples improved heat transfer by up to 19 %, depending on the dimple depth and *Re* number, while the friction factor is lowered 17.6 % more for the shallower dimples than for the pin fin arrays.

To summarize, altering the cross-sectional shape of pin fins and implementing the concept of hybrid pin/dimple arrays enhances the thermal–hydraulic performance of short pin fins. However, because they are millimeter scale, most of these arrays require intensive, complex, time-consuming, and unreasonably expensive manufacturing processes. From this perspective, NUCAP Industries Inc. has developed a proprietary skiving process which creates unique hook-shaped fins and corresponding dimples/cavities on metal surfaces (trademarked as GRIPMetal). Arrays of these features can be applied to the walls of longitudinal fins of heat sinks or heat exchangers or the inner/outer surfaces of tubes or serve as compact heat sinks themselves. These hook-shaped arrays represent an attractive surface enhancement technique because they are quick and simple to manufacture, have a relatively lower cost and, most importantly, are readily and commercially available in the market. Due to the nature of the skiving process, these features have a hook shape, heretofore referred to as hooks. These hooks offer increased surface area, enhance the turbulent mixing of the fluid, and/or promote boundary layer separation and three dimensionality of the flow field, which increases convective heat transfer. Their dimples increase the endwall mixing of the fluid by generating strong vortex flows.

The heat transfer performance of a liquid-to-air finned tube heat exchanger could be enhanced by the addition of an array of these hooks in the flow field. In addition, a cold plate enhanced with such features could also be an attractive cooling technology for modern power electronics such as IGBTs. However, the main challenge to design optimized, application-specific cooling technologies which leverage this novel surface enhancement is a lack of appropriate design tools or correlations that can predict heat transfer rates as a function of flow conditions and geometric parameters of the array. Therefore, the objective of the current work is to experimentally characterize the heat transfer and pressure drop of various arrays of hooks in a rectangular channel and evaluate their performance compared with that of a flat plate and existing short pin fin correlations. Variation of the clearance between the hook tip and the opposing endwall is also evaluated and investigated. This data will be used to develop correlations that can be used to facilitate the design of heat exchangers with GRIPMetal-enhanced surfaces.

2. Hook geometry

The hooks are manufactured by a skiving process and consist of material partially removed from the metal's surface. Thus, downstream or upstream of each hook there is a dimple/cavity from which the hooks were formed; thus, these dimples have an equal volume to the hooks. Depending on the depth of the tool, its angle of attack, and the stroke length, different hook sizes and arrays can be formed on the surface of a plate. A unit cell of a hook array, shown in Fig. 1, consists of two groups of hooks and each group has two adjacent hooks. Hooks 1 and 2 are separated by a clearance, C_h, and placed in a staggered arrangement with a streamwise pitch S_L. Hook 3 and Hook 4 are in the same arrangement as Hooks 1 and 2, but with a reversed orientation and at a spanwise pitch of S_T. Then, the array is formed by creating a rectangular pattern of unit cells in the streamwise and spanwise directions.

Fig. 2 shows the three different arrays of hooks that were tested, along with a magnified image for each array. The microscopic images were captured using a Leica MZ10 F stereomicroscope (Leica Microsystems GmbH, Wetzlar, Germany). The averaged normalized values of each array's geometrical parameters (height of hooks, spanwise pitch, streamwise pitch, etc.) are reported in Table 1 and explained in Fig. 3.

3. Experimental setup

3.1. Wind tunnel

Forced convection experiments were carried out in an open circuit wind tunnel using compressed air. The tunnel consists of the sections shown in Fig. 4. First, a diffuser section was connected by a hose to a pressure regulator placed on the compressed air line. This regulator sustains a constant inlet pressure to the tunnel during the experiments and, thus, a constant flowrate for a given Reynolds number. The diffuser had a diverging angle of 15° to minimize the turbulence and prevent flow separation from its walls. Second, a tube bundle section was attached to the diffuser for flow straightening, followed by an orifice setup for flow measuring. Finally, a contraction section was attached upstream of the developing section, which leads to the test section. All sections were 3D printed using PLA.

The test section is shown in Fig. 5. Here, the surfaces were tested in pairs; the hooked surfaces formed onto aluminum plates which faced each other to form a rectangular flow channel. Each pair had a different array of hooks (i.e., different geometrical parameters skived on their surfaces), corresponding to the hook arrays in Table 1. The plates were 50.8 mm wide and 101.6 mm long and manufactured from 3.175 mm thick aluminum.

Two copper heater blocks were each quipped with four 50 W cartridge heaters and were mechanically fastened to the base test plates to provide the necessary heat flux. Contact resistance was mitigated by using a thin layer of thermal paste ($k = 8.5$ W/mK) between the copper heater blocks and the aluminum test plates. All the remaining surfaces of the copper blocks were insulated with expanded polystyrene to minimize heat loss to the surroundings. Electrical power was provided to the heaters of each block independently and in equal amounts using a DC

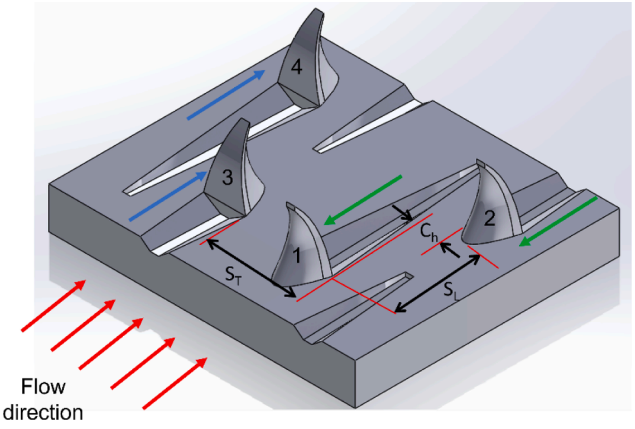

Fig. 1. A unit cell of a GRIPMetal array of hooks.

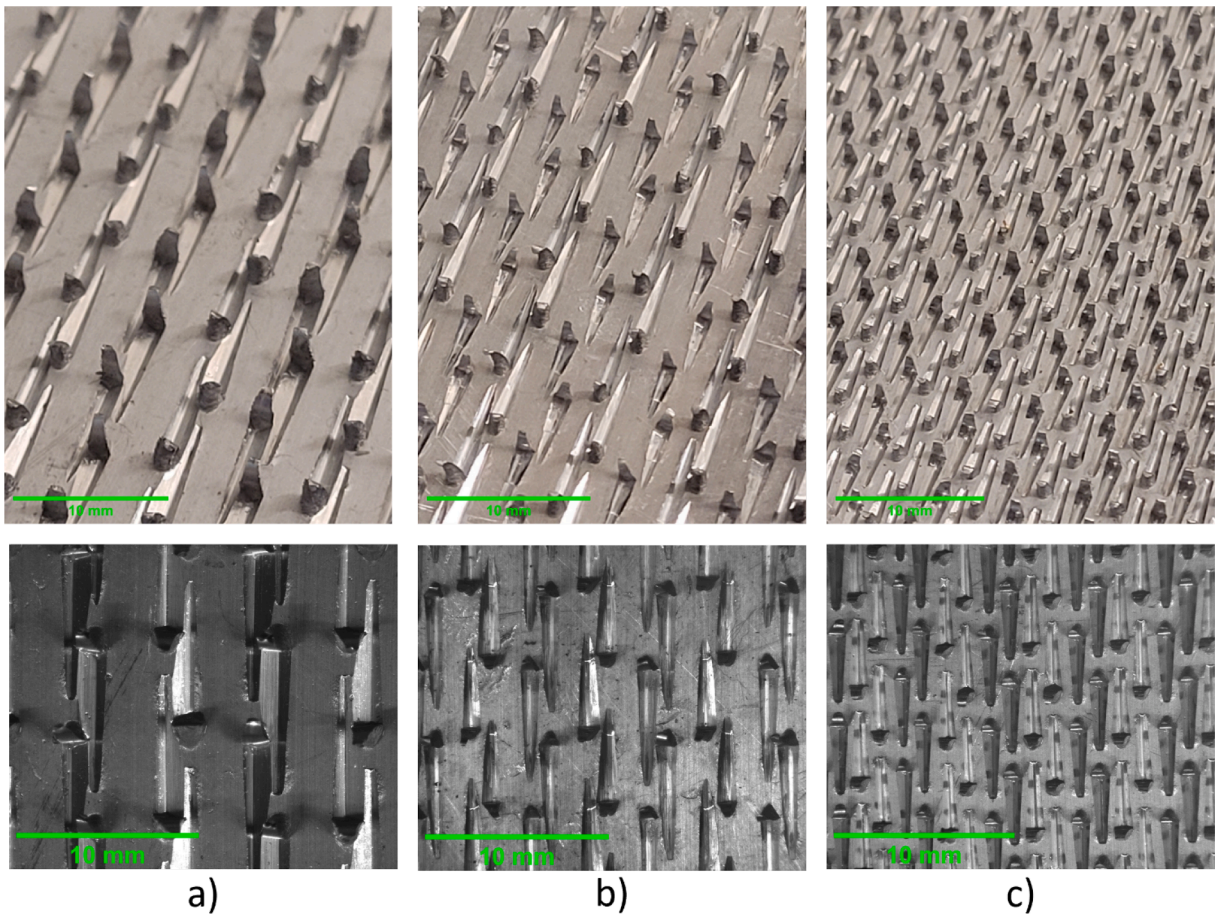

Fig. 2. Normal and microscopic images for tested arrays of hooks: a) heavy hooks b) standard hooks c) mini hooks.

Table 1
Normalized values of the geometrical parameters for different arrays of hooks.

#	Array Name	H (mm)	S_L/h	S_T/h	W_h/h	C_h/h	L_h/h	L_g/h
1	Standard	1.5	2.67	1.49	0.67	0.67	0.55	3.4
2	Mini	1	2.5	1.33	1	1	0.83	3.6
3	Heavy	2.25	1.78	1.69	0.71	0.44	0.67	3.33

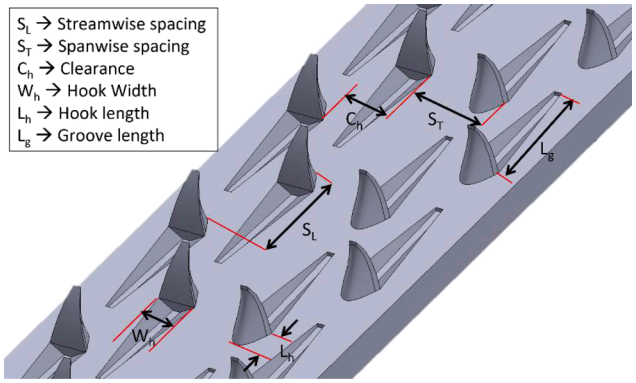

Fig. 3. Explanation of the geometrical parameters depicted in Table 1.

power supply (AIM-TTi CPX400DP). Power was controlled such that there was a temperature rise in the outlet air of 15 K with respect to the inlet (resulting in heat fluxes ranging from 0.19 to 1.9 W/cm^2). This temperature difference allowed for sufficient accuracy in the temperature difference between the tested plates and the air and was low enough to minimize thermal property variations in the test section and heat losses to the ambient. The air inlet bulk temperature was approximately 25 °C, while the wall temperature ranged from 30 °C to 60 °C, depending on the type of the surface being tested and the fluid flow rate.

Four 1.6 mm diameter *T*-type thermocouples were inserted into each aluminum plate 1.6 mm below the surface to measure the surface temperature distribution, as indicated in Fig. 5. Due to the high thermal conductivity of the aluminum and relatively low heat fluxes, the surface temperature, T_s, of the plate was approximately equal to the thermocouple readings. An additional thermocouple measured inlet air temperature, T_i. At the outlet, two thermocouples, of 0.8 mm diameter, were used to measure the approximate bulk fluid outlet temperature, T_o, and their relative positions are shown in Fig. 6.

The mass flow rate of the air was quantified using an orifice plate situated downstream of the fan section with properly sized upstream and downstream pipe lengths based on ASME PRC19.5 recommendations and [32]. Pressure taps were located at a distance of 25.4 mm upstream and downstream of the orifice plate and were connected differential pressure transducers, DPTs, (Amphenol All sensors BLVR series) to measure the pressure difference and calculate mass flow rate. For redundancy, variable area flowmeters were installed upstream of the wind tunnel and downstream of the pressure regulator to measure the volumetric flow rates. The readings from both methods were found to have negligible discrepancy within the measurement's uncertainties.

DPTs were also installed across the test section to measure its pressure drop. Four DPTs (Amphenol All sensors BLVR series) with different ranges of operating pressure were used, depending on the plate configuration and spacing. These DPTs were calibrated against an Omega PX409-001DWUI DPT which had an accuracy of 0.08 % of the full scale.

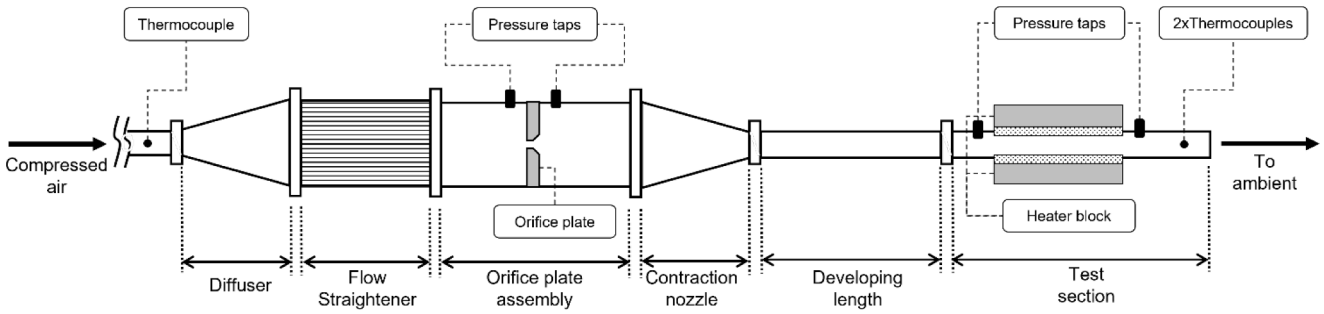

Fig. 4. Wind tunnel assembly details (not to scale).

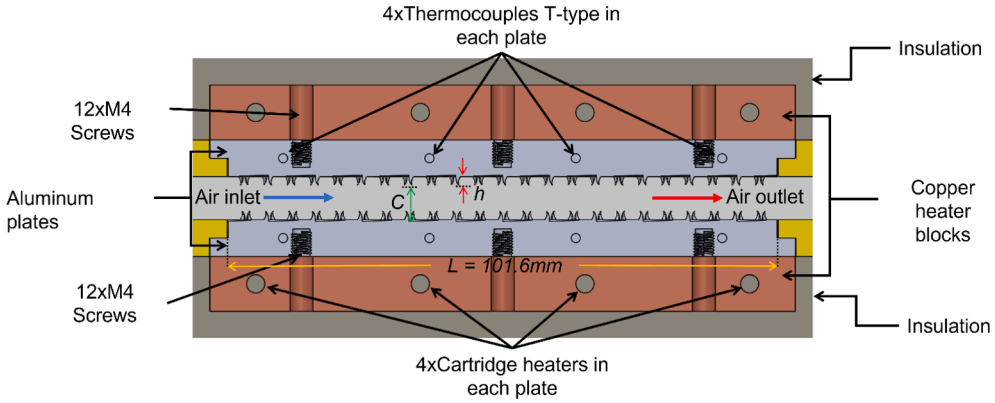

Fig. 5. Detailed cross section of the test section.

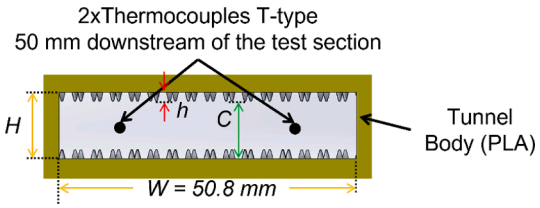

Fig. 6. Detailed position of the bulk fluid outlet temperature thermocouples.

Tests were conducted through a nominal Reynolds number based on the hydraulic diameter, *Re*, ranging from 4,000 to 20,000. Due to the nature of the implemented manufacturing technique, it is impractical to have the hooks of the two plates interdigitated. In addition, as discussed in the literature [21,22] the presence of tip clearance can potentially improve the performance of the array. Therefore, Standard hooks were tested at nominal tip clearances, $C = h, 2h, 4h$ and $6.5h$. Then, the other two types of hooks, (i.e., Mini and Heavy hooks) were tested at tip clearance values of $4h$ to evaluate the effect of changing the inter-fin spacings. This was achieved by changing the test section height, H, from 1.5 mm to 11.25 mm, according to the type of hooks being tested; this corresponds to an aspect ratio, H/W, of from 0.03 to 0.22. For comparison, at each test section height, a pair of flat plates was tested.

3.2. Heat loss calibration

Before running any test, heat loss to the surroundings was quantified by performing a series of calibration runs with no airflow in the test section. A PID controller was tuned to produce the approximate range of plate temperatures of interest. When steady state was reached, the input power, the average plate temperature, $T_{s,avg}$, and ambient temperature, T_{amb}, were measured so that an overall thermal resistance for the heat loss, R_{loss}, could be anticipated according to

$$Q_{loss} = \frac{\left(T_{s,avg} - T_{amb}\right)}{R_{loss}}. \quad (1)$$

Consequently, while running a test, the heat loss from the test section was calculated according to the measured plate and ambient temperatures using (1).

An energy balance was also performed on the test section to compare the energy gained by the air based on the measured temperature rise to that of the input energy introduced to the air by the heaters minus the heat loss. The error between the two energy values was evaluated. The average error was found to be 2.9 % for all the tested channels except H = 11.25 mm with most of the cases having an error of less than 9 %. The highest deviations were found to be for the H = 11.25 mm tunnel due to its relatively low fluid velocity that resulted in poor mixing of the fluid at the outlet and affected the outlet temperature measurements.

3.3. Data reduction & uncertainty analysis

In the current study, it was noted that the streamwise wall temperature gradient did not follow the constant heat flux distribution; instead, the gradient tended to be more isothermal. This behavior was more pronounced at low Nusselt numbers (i.e., low values of *Re* and/or wide tunnels). This can be attributed to the relatively high conductivity of the copper heater block and the aluminum test sections which offer a heat flow path in the axial direction that is an attractive alternative to that offered by the relatively low convection of air [33–39]. This axial conduction in the wall carries substantial amounts of heat in the opposite direction of the fluid flow, which tends to level out the temperature distribution. Therefore, the fluid exhibits a drastic rise in bulk temperature in the first portion of the test section. This is consistent with the findings of Maranzana et al. [35] who state that the bulk temperature profile is not linear. Consequently, the bulk temperature profile between the inlet and the outlet can be approximated to attain an exponential behavior and logarithmic temperature difference ΔT_{lm} which is adopted

and calculated as

$$\Delta T_{lm} = \frac{(T_{s,in} - T_i) - (T_{s,o} - T_o)}{ln(T_{s,in} - T_i) - ln(T_{s,o} - T_o)} \quad (2)$$

where $T_{s,in}$ and $T_{s,o}$ are, respectively, the inlet and outlet surface temperatures, obtained by linear extrapolation of the four thermocouple readings of each plate. Then, the overall heat transfer coefficient of an array of hooks, h_{lm}, was calculated for each plate as

$$h_{lm} = \frac{Q_{elec} - Q_{loss}}{A_b \Delta T_{lm}} \quad (3)$$

where Q_{elec} denotes the input electrical power to the heaters and A_b is the nominal area (101.6 × 50.8 mm^2). This form of h_{lm} reflects the heat transfer characteristics of the array as if there is a heat source mounted on the flat side of the plate, such as electronic-chip or plate heat exchangers. Finally, the average between the two plates was calculated, noting that the discrepancy between the values of h_{lm} for the two plates were found to be less than 7 %.

Another way of calculating the heat transfer coefficient employed in some studies [26,40–42] is to average the temperature difference between each thermocouple reading, $T_{s,i}$, for each plate and its corresponding local bulk air temperature, $T_{b,i}$ as

$$\Delta T_{bulk} = \frac{\sum_{i=1}^{4}(T_{s,i} - T_{b,i})}{4} \quad (4)$$

such that $T_{b,i}$ is calculated by assuming a linear rise of the air temperature along the test section. Then, the heat transfer coefficient, h_{bulk}, is calculated the same as h_{lm}, but replacing ΔT_{lm} with ΔT_{bulk} such that

$$h_{bulk} = \frac{Q_{elec} - Q_{loss}}{A_b \Delta T_{bulk}}. \quad (5)$$

The average difference between the calculated value of h between the two methods is 5 %; thus, only the first one is reported in this study.

It is common to present heat transfer results in the dimensionless form of a Nusselt number, Nu,

$$Nu = \frac{h_{lm} L_c}{k} \quad (6)$$

where k is the thermal conductivity of air at bulk temperature, which is equal to 0.0257 W/mK, while L_c is the characteristic length, which is either the fin height, h, or the hydraulic diameter of the channel, D_h, computed as

$$D_h = \frac{2(HW)}{H + W} \quad (7)$$

where H and W are the height and the width of the test section channel.

To characterize the pressure drop, the friction factor f is calculated as

$$f = \frac{2\,\Delta P\, L_c}{L_f\, V_{in}^2\, \rho} \quad (8)$$

where ρ is the density of air at bulk temperature, which is equal to 1.174 kg/m^3, ΔP is the difference across the test section measured by the DPT, and V_{in} is the mean inlet velocity to the test section.

Finally, the Reynolds number, Re, is calculated as

$$Re = \frac{\rho\, V_{in}\, D_h}{\mu} \quad (9)$$

where μ is the dynamic viscosity at air bulk temperature, which is equal to 1.861e^{-5} Pas.

For a comprehensive assessment of both heat transfer and pressure drop characteristics of the hooks compared to those of the flat plate, the overall thermal performance η (proposed by Gee and Webb [43]) is evaluated as

$$\eta = \frac{(Nu_{D_h}/Nu_o)}{(f_{D_h}/f_o)^{1/3}} \quad (10)$$

where Nu_o and f_o are the Nusselt number and the friction factor based on D_h for flat surfaces, respectively, and Nu_{Dh} and f_{Dh} are the Nusselt number and the friction factor based on D_h for channels with hooks, respectively.

The uncertainty of each parameter is evaluated based on the propagation method proposed by Kline and McClintock [44]. It was found that the maximum uncertainty in Re was 17 %. This occurred at low flow rates and narrow channels, while at higher flow rates and wide channels the uncertainty was lower than 4 %. For f, the maximum uncertainty at wide channels and low flow rates was up to 60 % and the minimum was 8 %. Regarding the Nu, the maximum uncertainty was 3 %.

4. Results

4.1. Comparison of flat plate to correlations

Fig. 7 compares heat transfer results for flat surfaces at different channel heights with two different correlations for turbulent heat transfer in a duct. The first correlation is the well-known Dittus–Boelter correlation [45] given by

$$Nu = 0.023\, Re^{0.8} Pr^{0.4} \quad (11)$$

The correlation is then multiplied by a correction factor to account for the thermally developing flow [5,46] as

$$Nu = 0.023\, Re^{0.8} Pr^{0.4} \left[1.11 \left(\frac{Re^{0.2}}{(L/D_h)^{0.8}}\right)^{0.275}\right] \quad (12)$$

for $L/L_d < 1$ and

$$Nu = 0.023\, Re^{0.8} Pr^{0.4} \left[1 + \frac{0.144\, Re^{0.25}}{L/D_h}\right] \quad (13)$$

for $L/L_d > 1$ and such that L_d is the developing length given by

$$L_d = 0.693\, Re^{0.25} D_h \quad (14)$$

The second correlation for comparison is the Petukhov correlation, modified by Gnielinski [27,28]:

$$Nu = \left(\frac{f/8*(Re - 1000)*Pr}{1 + 12.7\sqrt{f/8}*(Pr^{2/3} - 1)}\right)\left(1 + \frac{D_h}{L}^{2/3}\right) \quad (15)$$

where the friction factor, f, is calculated by Haaland correlation [49] given by

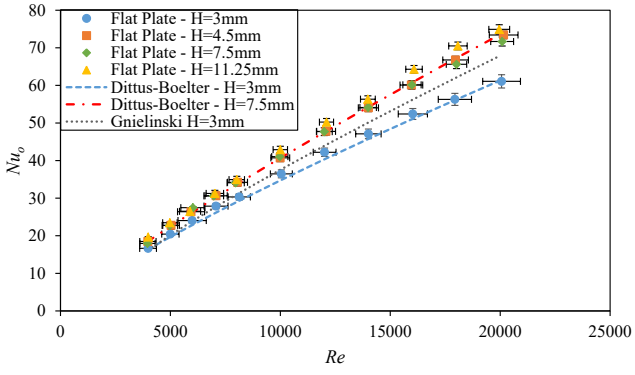

Fig. 7. Comparison of current facility's flat plate Nu number with correlations (11) & (15).

$$\frac{1}{\sqrt{f}} = -1.8\log\left(\left[\frac{\varepsilon/D_h}{3.7}\right]^{1.11} + \frac{6.9}{Re^*}\right) \quad (16)$$

such that Re^* is the modified Reynolds number proposed by Jones [50] to ensure a geometrical similarity between circular ducts and rectangular channels in calculating the friction factor given by

$$Re^* = \left[\frac{2}{3} + \frac{11H}{24W}\left(2 - \frac{H}{W}\right)\right]Re. \quad (17)$$

The experimental results for H = 3 mm spacing agrees well with the corrected Dittus–Boelter correlation and deviates from the Gnielinski correlation by only 8 % to 16 %. For channels H = 7.5 mm and 11.25 mm, the experimental *Nu* values are almost equal over the whole range of *Re* which is in good agreement with the corrected Dittus–Boelter correlation. We conjecture that this is mainly because the flow is thermally developing over the flat plates for those channels. The H = 3 mm channel has a thermally developing region that ranges from 30 % to 45 % of the plate length depending on *Re*; hence, it shows lower *Nu* than the other channels.

Fig. 8 compares the friction factor results for flat surfaces at two different channel heights with the Haaland correlation. The discrepancy between the experimental results and the correlation is 6 %–11 % within the *Re* range. For the H = 4.5 mm channel, the correlation overpredicted the friction factor. For the H = 3 mm channel, the correlation underpredicted the friction factor. We attribute this to the relatively large uncertainties in the velocity measurements, the characteristic dimension of the relatively small channel, and the roughness of the channel walls. In addition, the very high-aspect ratio of the rectangular channels increases the friction factor beyond the flat-plate correlation.

Overall, the heat transfer and pressure loss measurements for the flat plates are reasonable given the high-aspect ratio channel shape and thermally developing region for large spacings.

4.2. Effect of tip clearance

The variation of the Nusselt number of the GRIPMetal Standard hooks array with *Re* for the four tip clearances is shown in Fig. 9. Nu_h decreases with increasing clearance-to-fin-height ratio, *C/h*, at any given *Re*. This is primarily for two reasons: First, the increase in *C/h* is achieved by increasing the channel height, thus lowering the approach velocity at the same *Re*. Second, increasing *C/h* creates a lower resistance path for the flow; consequently, more flow will bypass the array, resulting in the array being washed by lower velocity flow. For all cases, Nu_h follows an increasing trend with *Re*. It should also be noted that with increasing *C/h*, the Nu_h becomes less dependent on *Re,* and it tends to reach an asymptotic value. This indicates that at relatively high *C/h* the hooks represents boundary layer roughness that enhances the heat

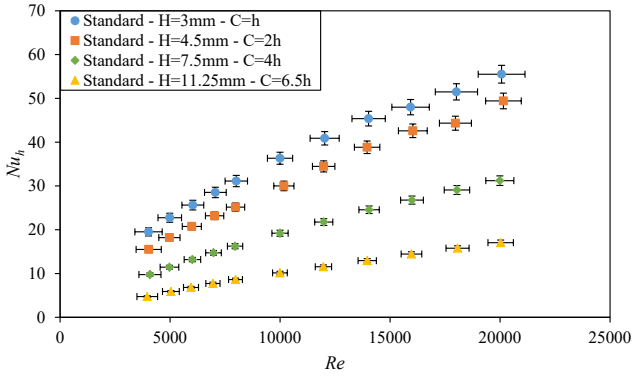

Fig. 9. Nu_h vs Re for rectangular channels with array of Standard hooks at different values of C/h.

transfer; this is consistent with the findings of Garimella and Eibeck [19].

Fig. 10 shows the ratio between hydraulic diameter Nusselt number, Nu_{Dh}, for the array of GRIPMetal Standard hooks and the Nusselt number for flat plate, Nu_o, at various tip clearances. At each tip clearance, a comparison is carried out with the flat plate at the same channel height. Thus, the hydraulic diameter is the constant for any given channel. Therefore, this ratio represents the heat transfer augmentation factor due to the presence of the array hooks. This augmentation is due to i) the addition of more heat transfer surface area which is 20–25 % more than the flat plate area, and ii) the enhanced fluid mix and promoting boundary layer separation. This ratio is greater than unity for all tested channels, indicating that the presence of these arrays enhanced heat transfer. Based on the literature, we conjecture that this enhancement can be attributed to the occurrence of the following phenomena in the flow field [10,51–54]: i) the presence of horseshoe vortices at the hook–endwall junction upstream of the hook that enhances three-dimensional advection in the flow, ii) the existence of secondary flows due to the vortex pairs shedding from two transverse rims of the dimple which increases the turbulence mixing intensity near the endwall downstream of the dimple, iii) the flow attachment and impingement in the trailing rim of the dimple, and iv) the promotion of turbulence mixing in the main bulk flow due to the shear layers separated from the tip of the hooks.

Except for *C/h* = 6.5, this ratio is the highest at low *Re*; then, it decreases with increasing *Re* approaching an asymptotic value. This occurs as the flow regime over the flat plate changes from transition to fully turbulent, i.e., increasing the heat transfer capability of the flat plates. Maximum enhancement in heat transfer is found for the *C/h* = 2 and *C/h* = 4 cases, with a factor of 4.6 at low flow rates and 3.75 at higher flow rates. The *C/h* = 1 case shows a slightly lower augmentation factor than

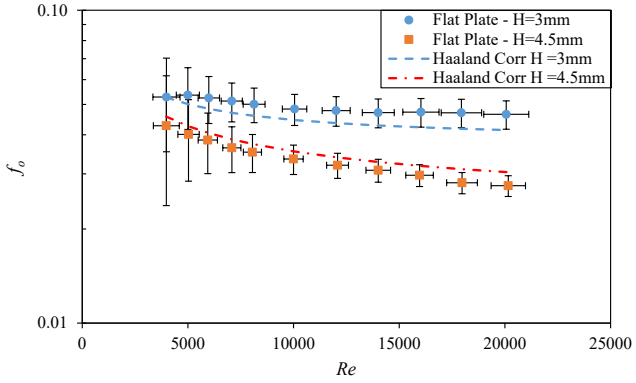

Fig. 8. Comparison of current facility's flat plate friction factor with correlation (16).

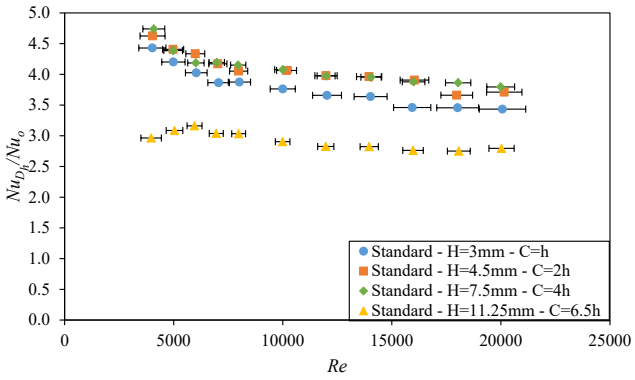

Fig. 10. Nu_h / Nu_o vs Re for rectangular channels with array of Standard hooks at different values of C/h.

the two latter cases; the factor is 4.45 and 3.45 at low and high flow rates, respectively. For $C/h = 6.5$, the flow sees the array of hooks as boundary layer roughness, i.e., at such relatively high clearance the plate is acting more like a roughened plate than the benchmark flat plate. Consequently, the augmentation factor maintains a relatively constant value of 3, regardless of the *Re*. This represents the lowest enhancement for all tested tip clearances, as expected.

Fig. 11 depicts the friction factor, f_h, for an array of GRIPMetal Standard hooks with varying tip clearances at different *Re*. Over the whole range of *Re*, the channel with $C/h = 1$ shows the greatest friction factor. This is logical because in this case the two opposing hooks are touching at the tips (i.e., no gap is present between the two hooks for flow). Therefore, the fluid is forced to flow entirely through the hooks array itself, which imposes very high restriction. In addition, the small channel height requires relatively high velocities to achieve the same *Re* when compared with the other cases. As a result, the velocity of the flow within the array is very high, producing more frictional losses. That is why the friction factor for this case follows a declining trend with *Re* because the frictional losses are dominant. On the other hand, the f_h values for the remaining arrays are much lower than the $C/h = 1$ case and are independent of *Re*. Here, increasing the tip clearance produces a gap with lower resistance to the flow, which consequently lowers the average flow velocities at a given *Re*. In addition, the bypass flow results in a lower velocity flow through the array itself, hence decreasing the skin friction between the hooks and the fluid, and the inertial losses become more significant. The dominance of the inertial losses over the frictional losses is the primary cause of the flattening of these curves [55].

Fig. 11 also shows the friction factor for a flat plate with a channel height of 11.25 mm, equivalent to the $C/h = 6.5$ case, calculated from Haaland's correlation (16), considering the roughness, ε, to be the fin height. The correlation is modified to account for the definition of f_h implemented in this study. The experimental results of f_h for the $C/h = 6.5$ case agree reasonably well with the values obtained from the empirical correlation. This further supports the conjecture that at such high values of C/h, the flow considers the array of hooks to be more like boundary layer roughness that increases the friction rather than as raised features.

For the final assessment of the performance of these different values of tip clearances, the overall thermal performance factor, η, was evaluated (shown in Fig. 12). According to the plot, within the studied *Re* range, η is independent of the value of C/h. In addition, as *Re* increases from 4,000 to 12,000, η gradually decreases from a value of 2.1 to 1.8, after which it also becomes independent of *Re*. Although the $C/h = 6.5$ showed a very low Nu_h compared with the other cases, having a friction factor that is comparable to a flat plate's resulted in the deterioration of its heat transfer capabilities. Having a $\eta > 1$ illustrates that the heat transfer enhancement provided by these hooks outweighs the pressure drop penalty.

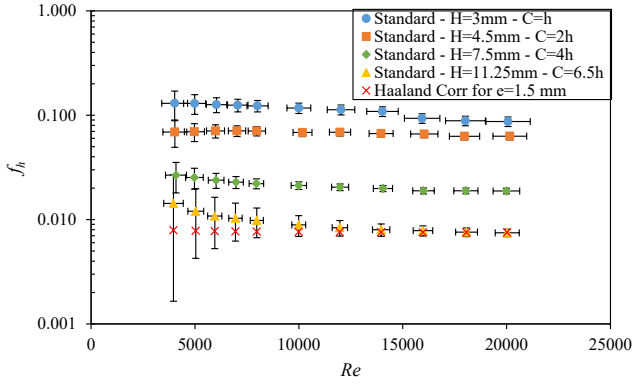

Fig. 11. f_h vs Re for rectangular channels with array of Standard hooks at different values of C/h.

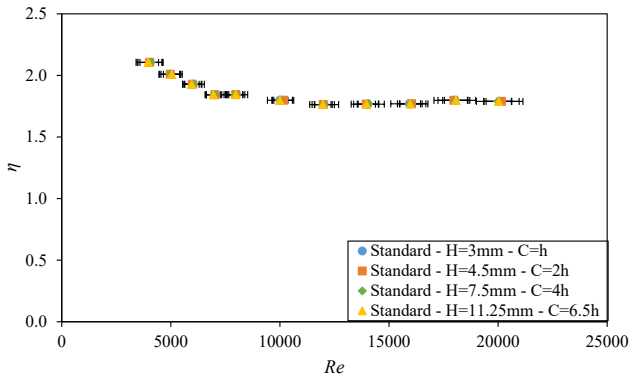

Fig. 12. η vs Re for rectangular channels with array of Standard hooks at different values of C/h.

One should carefully choose between these tip clearance values when implementing them in any given heat exchanger or heat sink application because having the same value of η can be deceiving. For instance, most electronics heat sinks or cold plates impose pressure drop constraints; thus, higher C/h values should be used, not lower ones. In this case, using a lower C/h value is not appropriate because it will incur a high pressure drop to the flow, lowering the *Re* and hence the Nu_h. On the other hand, choosing the high C/h value for its minimum pressure drop will yield a low heat transfer when applied in a particular heat exchanger and, hence, a higher surface temperature that might exceed design limitations.

4.3. Comparison with other surface enhancements

To the best of the authors' knowledge, no data on finned surfaces in the available literature captures the convective thermal–hydraulic performance of the present GRIPMetal arrays. This is because of i) the uniqueness of the proposed array in terms of the shape of the fin (hook-shaped) and its accompanying dimple, ii) the type of arrangement (i.e., changing orientation of the hooks and their dimple with respect to the flow from one column to another), and iii) the current rectangular channel is double-sided with arrays opposing each other. Nevertheless, comparisons of previously reported channels with state-of-the-art hybrid pin fin–dimple arrays [31] or dimple arrays [28,30] have been made to evaluate relative thermal–hydraulic performance.

Comparisons between hydraulic diameter based Nusselt number, Nu_{Dh}, and friction factor, f_{Dh} for a *Re* range of 8,000 to 20,000 were made. Fig. 13 shows the comparison of Nu_{Dh} for channels of GRIPMetal Standard hooks array at $C/h = 2$ and 6.5 with the heat transfer data from

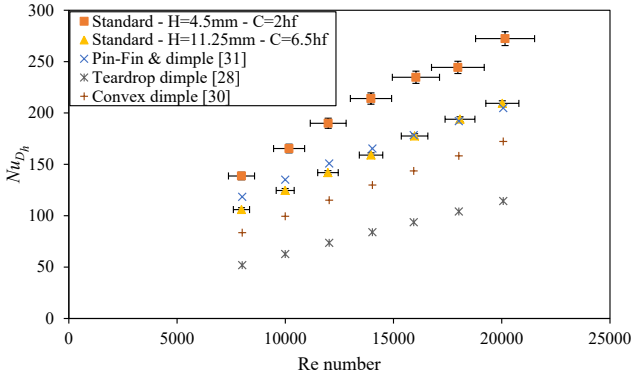

Fig. 13. Comparison of Nu_h between rectangular channels with array of Standard hooks C/h = 2 and 6.5, pin fin and dimple arrays from the existing literature.

[28,30,31]. Because the Nusselt number calculation in the present study is based on the nominal base area and not the heat transfer surface area, the reported Nusselt number for comparing studies was adjusted accordingly. First, a comparison between the GRIPMetal Standard hooks rectangular channel of C/h = 2 and the rectangular channel with the hybrid pin fin–dimple array of [31] seems relevant because they both have almost the same aspect ratio. It is seen in Fig. 13 that the GRIPMetal Standard hooks channel shows higher Nusselt number values than the other by 35–55 %, depending on *Re*. This can be contributed to the presence of a clearance between the two opposing hooks tips that induces severe vortex shedding and promotes turbulence in the main bulk flow because of the separated shear layers from those sharp hook tips [53]. Second, the dimples of the Standard hooks array can be approximated as the teardrop dimples investigated by Rao et al. [28]. Thus, the GRIPMetal Standard hooks channel of C/h = 6.5 was used for the comparison because it has an aspect ratio in the same magnitude as [28]. Also, the convex dimple studied by Gao et al. [30] was used for comparison because the dimples were applied to both endwalls of the channel as in the current study. From Fig. 13 we can conclude that the GRIPMetal Standard hooks array exhibits higher convective heat transfer than the dimple arrays within the compared range of *Re*, which is in good agreement with findings of Rao et al. [31].

In Fig. 14, f_{Dh} for channels of Standard hooks array at $C/h = 2$ and 6.5 is compared with the friction factors from previous studies. The friction factor of the channel $C/h = 2$ of the current study is lower than that of the channel with a hybrid pin fin–dimple array of [31] by about 45 %. One possible explanation for this is the presence of a gap between the two opposing plates which offers a lower resistance path to the flow; this consequently lowers the pressure drop at a given *Re* when compared with the hybrid pin fin–dimple array that filled the whole channel. On the other hand, the GRIPMetal channel of $C/h = 6.5$ has a friction factor that is 7 times the friction factor of the teardrop dimples [28] and 10 ~ 13 times that of the convex dimples [30]. This is mainly because the presence of the hooks obstructs the flow, creating a low-pressure area downstream of the hook and a high-pressure area upstream due to the stagnation of the flow. Although the presence of the dimple downstream of the hooks reduces the intensity of the wakes downstream of the hooks and, thus, reduces the pressure drop, this effect still did not counteract the drag imposed by the hooks.

4.4. Nusselt number correlations

The Nusselt number, Nu_h, in Fig. 9 was correlated through a nonlinear multiple variable regression analysis. The correlation took the following form as a function of *Re* and *C/h*:

$$Nu_h = a\,Re^b (C/h)^d Pr^{0.4} \tag{18}$$

where *Pr* is the Prandtl number of the air at the mean bulk temperature. Including *Pr* in the correlation will allow potential users to easily assess different fluids. An attempt was made to generate a single correlation for the four tested tip clearances; however, the correlation could not predict Nu_h accurately enough, especially for the $C/h = 6.5$ channel which had a root square mean error (RMSE) of 21 %. Consequently, an alternate definition of the Reynolds number is considered to correlate the experimental data; this is referred to as the array Reynolds number, Re_a. The distinction between the array Reynolds number and Eq.(9) is the usage of the array velocity, V_a, as a reference velocity instead of the mean inlet velocity, V_{in}. This Re_a was previously defined by Garimella and Eibeck [19]. The motivation for using the array velocity V_a, is as follows. The presence of the tip clearance, *C*, divides the flow into two streams: i) the bypass stream and ii) the array stream and their ratio depends on the value of *C* (i.e., the ratio between the pressure drops of these streams). Thus, the actual velocity affecting the heat transfer from the array is not the mean inlet velocity but, rather, the velocity to which the hooks are exposed (i.e., array velocity, V_a).

Because most of the pressure drop in the channel is due to the drag encountered by the presence of the hooks, the drag is the determining factor for the ratio between the array velocity and the mean inlet velocity. As the tip clearance increases, more flow bypasses the array, resulting in lower drag coefficient and indicating a decrease in the array velocity. Hence, the mean inlet velocity and the array velocity are related to each other through the drag coefficient of the hooks as

$$V_a = V_{in}\sqrt{C_{d,i}/C_{d,C=h}} \tag{19}$$

where C_d is the drag coefficient of an array of hooks defined by

$$C_d = \frac{2\,\Delta P}{V_{in}^2 \rho}. \tag{20}$$

Because the $C/h = 1$ case corresponds to the situation where there is no tip clearance between the two opposing plates (i.e., all the flow passes through the array), the drag coefficient of this channel, $C_{d,C=h}$, is used as the reference coefficient. Fig. 15 shows the drag coefficient for an array of Standard hooks with $C/h = 1$, 2, or 4 at different *Re* (the omission of C/h = 6.5 is discussed below).

After applying the definition of Re_a in the experimental data, the Nu_h for channels with *C/h* values of 1, 2, or 4 could be correlated to a single correlation. However, the prediction of Nu_h for $C/h = 6.5$ employing the Re_a definition did not produce an accurate correlation. This is because at such high values of tip clearances, the array affects the flow as surface roughness rather than as an array of raised features; thus, the array velocity V_a is no longer the effective velocity, and the heat transfer augmentation mechanism is different. Therefore, two sperate correlations were developed. The first,

$$Nu_h = 0.1063\,Re_a^{0.646}(C/h)^{-0.05371} Pr^{0.4} \quad \text{for} \quad 1 \le C/h \le 4 \tag{21}$$

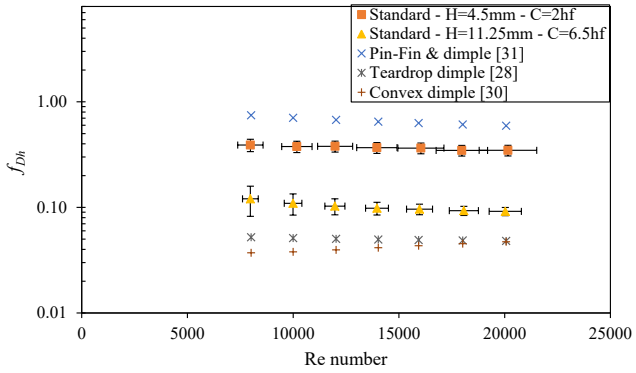

Fig. 14. Comparison of f_h between rectangular channels with array of Standard hooks C/h = 2 and 6.5, pin fin and dimple arrays from the existing literature.

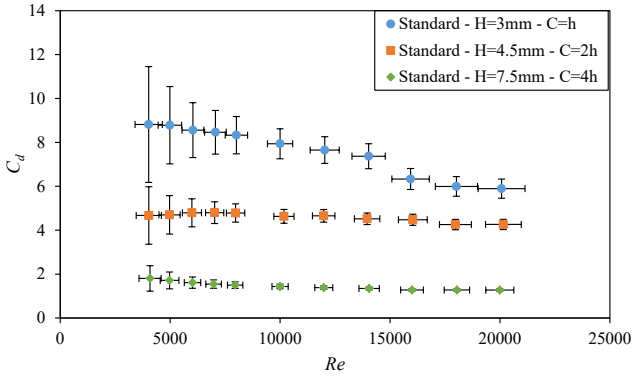

Fig. 15. C_d vs Re for rectangular channels with array of Standard hooks at different values of C/h.

is for channels with C/h values of 1, 2, or 4, implementing Re_a.

The other correlation,

$$Nu_h = 0.1542\,Re^{0.7301}(C/h)^{-1.286}Pr^{0.4} \quad \text{for} \quad 4 \le C/h \le 6.5 \tag{22}$$

is for the $C/h = 4$ or 6.5 channels using Re.

The presence of channel $C/h = 4$ in both correlations is to check the validity of (22) for intermediate values of C/h and to prove the adequacy of the proposed claims.

A comparison between the experimental data and the above-mentioned correlations is depicted in Fig. 16. The y-axis represents the Nu_h normalized by $Pr^{0.4}$ and $(C/h)^{n}$ in a log scale such that n is the exponent defined in correlations (21) and (22). The RMSE between predictions using these correlations and the experimental data is 3.7 % and 2.4 %, respectively. The collapse of the experimental data for channels with C/h values of 1, 2, or 4 on a single straight line helps justify the use of array velocity, V_a, as the physically significant reference velocity.

The value of Reynolds number's exponent of either 0.646 or 0.7301 shows that the convection through these arrays is dominated by strong turbulence and flow separation. The Reynolds number index for correlation (22) is higher, indicating that it exhibits lower dependency on the Reynolds number than (20). Also, it is approaching the 0.8 power dependence of the flat plate's heat transfer, supporting the claim that at high C/h values the flow is affected by these arrays as surface roughness.

The exponent of C/h for correlation (21) suggests that Nu_h for such arrays is not greatly affected by tip clearance; however, this is not the case because the effect of C/h is already included in the Re_a term. For correlation (22), the exponent C/h indicates that the effect of increasing C/h is to decrease the Nu_h; however, this effect declines with increasing C/h, indicates the possibility of using the same correlation for predicting the Nu_h for channels with C/h values greater than 6.5 wit ha reasonable accuracy.

4.5. Friction factor correlations

In addition to the Nusselt number, the friction factor, f_h, shown in Fig. 11 was correlated through performing nonlinear multiple variable regression analysis. Inspired by the friction factor correlations in the literature, the correlation took the following form as a function of Re and C/h:

$$f_h = \left[a\log Re + b(C/h)^{d}\right]^{n}. \tag{23}$$

Following the same procedure as above for correlating the Nu_h data, two separate correlations were developed for two different ranges of C/h. The first correlation,

$$f_h = \left[0.66\log Re + 0.363(C/h)^{1.763}\right]^{-2} \quad \text{for} \quad 4 \le C/h \le 6.5 \tag{24}$$

is for channels with C/h values of 1, 2, or 4.

The other correlation,

$$f_h = 0.01\left[-\log Re + 11.5(C/h)^{-0.451}\right] \quad \text{for} \quad 4 \le C/h \le 6.5 \tag{25}$$

is for the $C/h = 4$ or 6.5 channels.

The presence of channel $C/h = 4$ in both correlations is to check the validity of correlation (25) for intermediate values of C/h.

Fig. 17 shows a comparison of the experimental data of f_h with its corresponding predicted values implementing correlation (24) and (25). The RMSE between predictions using these correlations and the experimental data are 6.5 % and 5.3 %, respectively.

4.6. Effect of hook geometry

In this section, the effect of streamwise and spanwise spacings between hooks and the hook size on the heat transfer and pressure drop characteristics is evaluated. To this end, two additional arrays of "Heavy" and "Mini" hooks (see geometrical parameters given in Table 1) were tested at tip-clearance-to-height ratio $C/h = 4$. Fig. 18 shows the Nu_h for three different arrays of Standard, Heavy and Mini hooks at $C/h = 4$ over the range of Re. As expected, the Nu_h increases with Re irrespective of the hook type. Results for the three types of hooks are shown as collapsing onto a single straight line, with a slight difference between the Heavy hooks and the others of only about 3 %. This indicates that at this C/h value and above, inter-fin spacings and hook shape have limited influence on the heat transfer of these arrays. It also shows that the choice of hook height as the characteristic length is appropriate. Thus, the correlations provided in Section 4.4 could be applied to the other types of hooks for $C/h \ge 4$.

On the other hand, Fig. 19 represents the change of friction factor, f_h, for the three tested types of hooks at $C/h = 4$ with Re. It should be noted that, regardless of the value of Re, the Mini hooks array exhibits the greatest friction factor by a factor of 2.2 compared with the Standard hooks. This increase in f_h is attributed to two factors: First, to achieve $C/h = 4$ for Mini hooks, the channel height is reduced to 5 mm while the Standard and Heavy hooks require a height of 7.5 mm and 11.25 mm, respectively. This height results in a 33 % reduction in the flow area compared with that of the Standard hooks case and, therefore, at any given Re, the approach velocity is the highest for Mini hooks. Second, the Mini hook array has spanwise spacings that are almost half those of the Standard and Heavy hooks arrays. As previously stated, and as found in [15–17], the pressure loss is greatly affected by spanwise spacing as a direct result of flow restriction between the hooks.

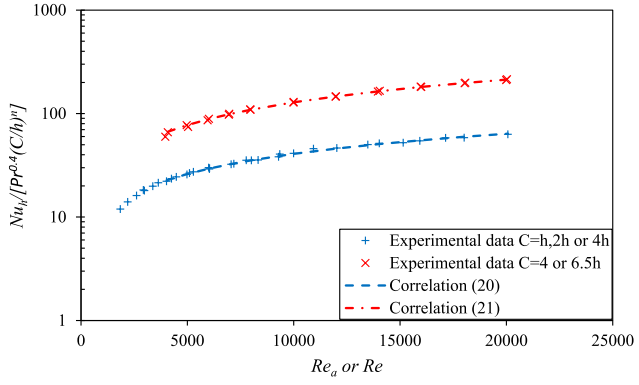

Fig. 16. Comparison between correlations of Nu_h and experimental data for Standard hooks array.

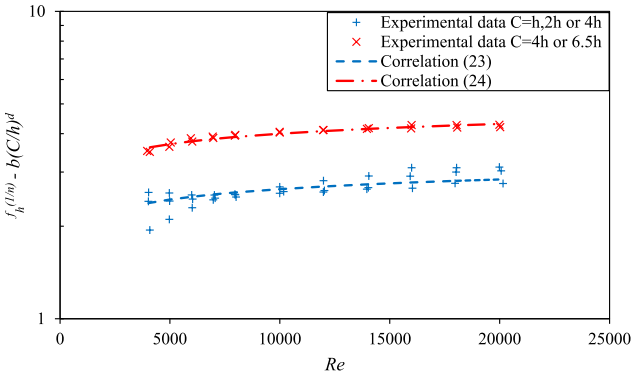

Fig. 17. Comparison between correlations of f_h and experimental data for Standard hooks array.

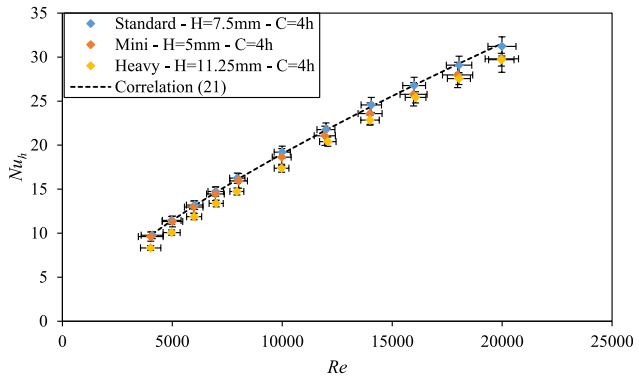

Fig. 18. Nu_h vs Re for rectangular channels with arrays of different types of hooks at C/h = 4.

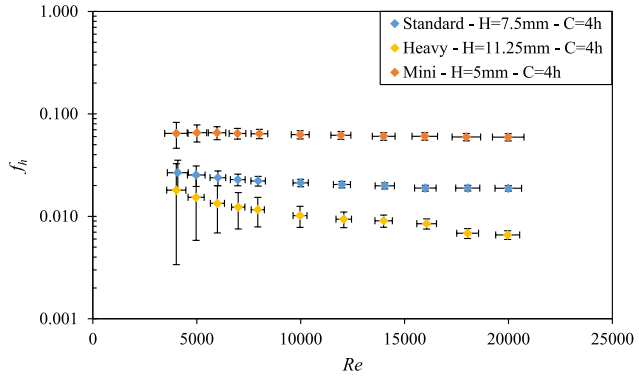

Fig. 19. f_h vs Re for rectangular channels with arrays of different types of hooks at C/h = 4.

5. Summary & conclusions

In this study, the thermal and hydrodynamic performance of arrays of hook-shaped raised features and dimples on metal surfaces (GRIPMetal) developed by NUCAP Industries Inc. was experimentally characterized and compared with flat plates to develop predictive correlations to serve as design tools for heat exchanger applications. Such arrays are an attractive option for convective heat transfer enhancement due to their manufacturing simplicity and speed, low cost, and commercial availability in the market.

The effect of tip clearance, C, for an array of GRIPMetal Standard hooks with a nominal height, $h = 1.5$ mm, was investigated at values of h, 2 h, 4 h, 6.5 h. Then, two more arrays with hooks of $h = 1$ mm and $h = 2.25$ mm, and different inter-fin spacings were tested at $C/h = 4$. Results were obtained at Reynolds numbers ranging from 4,000 to 20,000 using air as the working fluid. The results show that these hooks have good potential for practical air-side heat transfer enhancement and the following conclusions can be drawn:

- The array of Standard hooks improved the heat transfer capabilities of the rectangular channel depending on the value of tip-clearance-to-fin-height ratio, C/h. Maximum enhancement in heat transfer was found to be for $C/h = 2$ and $C/h = 4$ cases with a factor of 4.6 at low flow rates and 3.75 at higher ratios.
- A comparison of Nu_h for Standard hooks with the flat plate, Nu_o, at various tip clearance values showed that the heat transfer augmentation due to the presence of the hooks is the highest at low Re, then it decreases with increasing Re for the $C/h = 2$ and $C/h = 4$ cases by a factor of 4.6. While for $C/h = 6.5$ the enhancement maintains a relatively constant factor of 3 regardless of the Re.
- The Nusselt number decreases with increasing tip-clearance-to-fin-height ratio, C/h, at any given Re approaching an asymptotic value at higher C/h ratios, which is consistent with [18].
- The friction factor, f_h, of the channel with tip-clearance-to-fin-height ratio, $C/h = 1$, is the greatest with a declining trend with Re. However, for the remaining values of C/h, the friction factors are much lower and are independent of Re. This f_h - Re curve flattening is consistent with [38].
- The experimental results of f_h for the $C/h = 6.5$ case are coincident with the values obtained from Haaland's correlation [36]. This reinforces the claim that at such high values of C/h, the array of hooks act as boundary layer roughness rather than as raised features.
- The heat transfer performance of GRIPMetal Standard hooks array was found to be higher than performance data available in the literature for a hybrid staggered pin fin–dimple array, teardrop dimples staggered array, and convex dimple staggered array. On the other hand, GRIPMetal Standard hooks arrays exhibited pressure drop characteristics higher than both dimple arrays and lower than the hybrid staggered pin fin–dimple array.
- Two distinct correlations were developed for the Nu_h as a function of the array Reynolds number, Re_a, and tip-clearance-to-height ratio, C/h. Also, two correlations were obtained for the friction factor as a function of Reynolds number, Re, and tip-clearance-to-height-ratio, C/h. These four correlations can be used as design tools to employ these hooks in any given application.
- The overall thermal performance factor, η, is independent of the value of C/h within the range of Re investigated. It steadily declines from 2.1 to 1.8 as Re increases from 4,000 to 12,000; then, it becomes independent of Re. These hooks have $\eta > 1$ which demonstrates that the heat transfer enhancement offsets the pressure drop penalty.
- Geometrical parameters of such arrays of hooks (i.e., hook height and streamwise and spanwise spacings between them) is found to have no effect on heat transfer characteristics at $C/h = 4$. Therefore, the developed correlations of Nu_h for Standard hooks can be used for the other two types for $C/h \geq 4$.
- The friction factor, f_h, of the Mini hooks array showed higher values than that of Standard and Heavy hooks arrays at any given Re. This can be attributed to i) the array's approach velocity is the highest for Mini hooks; and ii) the Mini hooks array has a spanwise spacing that is almost half that of the Standard and Heavy hooks arrays.

Future work will explore the application of these GRIPMetal-enhanced surfaces to real-world heat exchanger applications.

Declaration of Competing Interest

The authors declare that they have no known competing financial interests or personal relationships that could have appeared to influence the work reported in this paper.

Acknowledgments

The authors gratefully acknowledge the support of the Natural Sciences and Engineering Research Council of Canada (NSERC) grant number ALLRP 552123-20.

References

[1] A. Sakanova, K.J. Tseng, Comparison of pin-fin and finned shape heat sink for power electronics in future aircraft, Appl. Therm. Eng. 136 (2018) 364–374, https://doi.org/10.1016/j.applthermaleng.2018.03.020.
[2] L. Chen, R.G.A. Brakmann, B. Weigand, R. Poser, Q. Yang, Detailed investigation of staggered jet impingement array cooling performance with cubic micro pin fin roughened target plate, Appl. Therm. Eng. 171 (2020), 115095, https://doi.org/10.1016/j.applthermaleng.2020.115095.
[3] F.Z. Bakhti, M. Si-Ameur, A comparison of mixed convective heat transfer performance of nanofluids cooled heat sink with circular perforated pin fin, Appl.

Therm. Eng. 159 (2019), 113819, https://doi.org/10.1016/j.applthermaleng.2019.113819.
[4] V. Choudhary, M. Kumar, A.K. Patil, Experimental investigation of enhanced performance of pin fin heat sink with wings, Appl. Therm. Eng. 155 (2019) 546–562, https://doi.org/10.1016/j.applthermaleng.2019.03.139.
[5] G.J. VanFossen, Heat transfer coefficients for staggered arrays of short pin fins, Proc. ASME Turbo Expo (1981), https://doi.org/10.1115/81-GT-75.
[6] E.M. Sparrow, J.W. Ramsey, Heat transfer and pressure drop for a staggered wall-attached array of cylinders with tip clearance, Int. J. Heat Mass Transf. 21 (1978) 1369–1378, https://doi.org/10.1016/0017-9310(78)90200-4.
[7] D.E. Metzger, R.A. Berry, J.P. Bronson, Developing heat transfer in rectangular ducts with arrays of short pin fins, in: Am. Soc. Mech. Eng., 1981.
[8] J. Armstrong, D. Winstanley, A review of staggered array pin, J. Turbomach. 110 (1988) 94–103.
[9] O.N. Sßara*, Performance analysis of rectangular ducts with staggered square pin fins, Energy Convers. Manage. 44 (2003) 1787–1803. https://doi.org/10.1016/S0140-6701(03)92683-X.
[10] M.K. Chyu, V. Natarajan, Heat transfer on the base surface of three-dimensional protruding elements, Int. J. Heat Mass Transf. 39 (1996) 2925–2935, https://doi.org/10.1016/0017-9310(95)00381-9.
[11] M.K. Chyu, Heat transfer and pressure drop for short pin-fin arrays with pin-endwall fillet, Proc. ASME Turbo Expo. 4 (1989), https://doi.org/10.1115/89-GT-99.
[12] M.K. Chyu, Y.C. Hsing, T.I.P. Shih, V. Natarajan, Heat transfer contributions of pins and endwall in pin-fin arrays: effects of thermal boundary condition modeling, J. Turbomach. 121 (1999) 257–263, https://doi.org/10.1115/1.2841309.
[13] M.K. Chyu, R.J. Goldstein, Influence of an array of wall-mounted cylinders on the mass transfer from a flat surface, Int. J. Heat Mass Transf. 34 (1991) 2175–2186, https://doi.org/10.1016/0017-9310(91)90044-F.
[14] E.M. Sparrow, J.W. Ramsey, C.A.C. Altemani, Experiments on in-line pin fin arrays and performance comparisons with staggered arrays, J. Heat Transfer. 102 (1980) 44–50, https://doi.org/10.1115/1.3244247.
[15] S.A. Lawson, A.A. Thrift, K.A. Thole, A. Kohli, Heat transfer from multiple row arrays of low aspect ratio pin fins, Int. J. Heat Mass Transf. 54 (2011) 4099–4109, https://doi.org/10.1016/j.ijheatmasstransfer.2011.04.001.
[16] K.K. Ferster, K.L. Kirsch, K.A. Thole, Effects of geometry, spacing, and number of pin fins in additively manufactured microchannel pin fin arrays, J. Turbomach. 140 (2018) 1–10, https://doi.org/10.1115/1.4038179.
[17] M.E. Lyall, A.A. Thrift, K.A. Thole, A. Kohli, Heat transfer from low aspect ratio pin fins, J. Turbomach. 133 (2011), https://doi.org/10.1115/1.2812951.
[18] E.M. Sparrow, D.S. Kadle, Effect of tip-to-shroud clearance on turbulent heat transfer from a shrouded, longitudinal fin array, J. Heat Transfer. 108 (1986) 519–524, https://doi.org/10.1115/1.3246965.
[19] S.V. Garimella, P.A. Eibeck, Heat transfer characteristics of an array of protruding elements in single phase forced convection, Int. J. Heat Mass Transf. 33 (1990) 2659–2669, https://doi.org/10.1016/0017-9310(90)90202-6.
[20] B.A. Jubran, M.A. Hamdan, R.M. Abdualh, Enhanced heat transfer missing pin, and optimization for cylindrical pin fin arrays, J. Heat Transfer. 115 (1993) 576–583, https://doi.org/10.1115/1.2910727.
[21] K.A. Moores, Y.K. Joshi, Effect of tip clearance on the thermal and hydrodynamic performance of a shrouded pin fin array, J. Heat Transfer. 125 (2003) 999–1006, https://doi.org/10.1115/1.1621897.
[22] H. Tabkhi, A. Nayebzadeh, Y. Peles, Experimental and numerical local heat transfer study on micro pin fin with tip clearance, Appl. Therm. Eng. 179 (2020), 115756, https://doi.org/10.1016/j.applthermaleng.2020.115756.
[23] M. D, C. Fan, S. Haley, Effects of pin shape and array orientation on heat transfer and pressure loss in pin fin arrays, J. Eng. Gas Turbines Power. 106 (1984) 252–257. https://doi.org/10.1115/GT2010-23227.
[24] M.K. Chyu, Y.C. Hsing, V. Natarajan, Convective heat transfer of cubic fin arrays in a narrow channel, J. Turbomach. 120 (1998) 362–367, https://doi.org/10.1115/1.2841414.
[25] N. Sahiti, A. Lemouedda, D. Stojkovic, F. Durst, E. Franz, Performance comparison of pin fin in-duct flow arrays with various pin cross-sections, Appl. Therm. Eng. 26 (2006) 1176–1192, https://doi.org/10.1016/j.applthermaleng.2005.10.042.
[26] J. Xi, J. Yao, P. Su, J. Lei, J. Wu, T. Gao, Heat transfer and pressure loss characteristics of Pin-Fins with Different Shapes in a wide channel, in: Proc. ASME Turbo Expo, 2017: pp. 1–9. https://doi.org/10.1115/GT2013-95407.
[27] M.K. Chyu, Y. Yu, H. Ding, J.P. Downs, F.O. Soechting, Concavity Enhanced Heat Transfer in an Internal Cooling Passage, in: Vol. 3 Heat Transf. Electr. Power; Ind. Cogener., American Society of Mechanical Engineers, 1997: pp. 1–7. https://doi.org/10.1115/97-GT-437.
[28] Y. Rao, Y. Feng, B. Li, B. Weigand, Experimental and numerical study of heat transfer and flow friction in channels with dimples of different shapes, J. Heat Transfer. 137 (2015) 1–10, https://doi.org/10.1115/1.4029036.
[29] H.K. Moon, T. O'Connell, B. Glezer, Channel height effect on heat transfer and friction in a dimpled passage, Proc. ASME Turbo Expo. 3 (1999) 307–313, https://doi.org/10.1115/99-GT-163.
[30] Y. Gao, Y. Feng, K. Tang, P. Hrnjak, Experimental study on forced convection hydraulic and thermal characteristics in a dimpled flat duct, Appl. Therm. Eng. 181 (2020), 115921, https://doi.org/10.1016/j.applthermaleng.2020.115921.
[31] Y. Rao, C. Wan, Y. Xu, An experimental study of pressure loss and heat transfer in the pin fin-dimple channels with various dimple depths, Int. J. Heat Mass Transf. 55 (2012) 6723–6733, https://doi.org/10.1016/j.ijheatmasstransfer.2012.06.081.
[32] R.W. Miller, Flow measurement engineering handbook, 1983.
[33] E.J. Davis, W.N. Gill, The effects of axial conduction in the wall on heat transfer with laminar flow, Int. J. Heat Mass Transf. 13 (1970) 459–470, https://doi.org/10.1016/0017-9310(70)90143-2.
[34] M. Faghri, E.M. Sparrow, Simultaneous wall and fluid axial conduction in laminar pipe-flow heat transfer, J. Heat Transfer. 102 (1980) 58–63, https://doi.org/10.1115/1.3244249.
[35] G. Maranzana, I. Perry, D. Maillet, Mini- and micro-channels: Influence of axial conduction in the walls, Int. J. Heat Mass Transf. 47 (2004) 3993–4004, https://doi.org/10.1016/j.ijheatmasstransfer.2004.04.016.
[36] G.S. Barozzi, G. Pagliarini, A method to solve conjugate heat transfer problems: the case of fully developed laminar flow in a pipe, J. Heat Transfer. 107 (1985) 77–83, https://doi.org/10.1115/1.3247406.
[37] B. Weigand, G. Gassner, The effect of wall conduction for the extended Graetz problem for laminar and turbulent channel flows, Int. J. Heat Mass Transf. 50 (2007) 1097–1105, https://doi.org/10.1016/j.ijheatmasstransfer.2006.06.047.
[38] S. Mikio, E. Kazuo, Effect of conduction in wall on heat transfer with turbulent flow between parallel plates, Int. J. Heat Mass Transf. 20 (1977) 507–516, https://doi.org/10.1016/0017-9310(77)90097-7.
[39] R.K. Shah, A.L. London, Laminar Flow Forced Convection in Ducts: A Source Book for, Compact Heat Exchanger Analytical Data (1978). http://www.sciencedirect.com/science/article/pii/B978012020051150022X.
[40] M.K. Chyu, E.O. Oluyede, H.K. Moon, Heat transfer on convective surfaces with pin-fins mounted in inclined angles, Proc. ASME Turbo Expo. 4 PART B (2007) 861–869. https://doi.org/10.1115/GT2007-28138.
[41] S.C. Siw, A.D. Fradeneck, M.K. Chyu, M.A. Alvin, The effects of different pin-fin arrays on heat transfer and pressure loss in a narrow channel, in: Proc. ASME Turbo Expo, 2015: pp. 1–9. https://doi.org/10.1115/GT2015-43855.
[42] G. Tanda, Heat transfer and pressure drop in a rectangular channel with diamond-shaped elements, Int. J. Heat Mass Transf. 44 (18) (2001) 3529–3541.
[43] D.L. Gee, R.L. Webb, Forced convection heat transfer in helically rib-roughened tubes, Int. J. Heat Mass Transf. 23 (1980) 1127–1136, https://doi.org/10.1016/0017-9310(80)90177-5.
[44] S.J. Kline, Describing uncertainty in single sample experiments, Mech. Eng. 75 (1953) 3–8.
[45] F.W. Dittus, L.M.K. Boelter, Heat transfer in automobile radiators of the tubular type, Int. Commun. Heat Mass Transf. 12 (1985) 3–22, https://doi.org/10.1016/0735-1933(85)90003-X.
[46] W.H. McAdams, Heat Transmission, 3d Ed, McGraw-Hill, 1954.
[49] S.E. Haaland, Simple and explicit formulas for the friction factor in turbulent pipe flow, J. Fluids Eng. Trans. ASME. 105 (1983) 89–90, https://doi.org/10.1115/1.3240948.
[50] O.C. Jones, An improvement in the calculation of turbulent friction in rectangular ducts, J. Fluids Eng. 98 (1976) 173–180, https://doi.org/10.1115/1.3448250.
[51] G.I. Mahmood, M.L. Hill, D.L. Nelson, P.M. Ligrani, H.K. Moon, B. Glezer, Local heat transfer and flow structure on and above a dimpled surface in a channel, J. Turbomach. 123 (2001) 115–123, https://doi.org/10.1115/1.1333694.
[52] G.I. Mahmood, P.M. Ligrani, Heat transfer in a dimpled channel: Combined influences of aspect ratio, temperature ratio, Reynolds number, and flow structure, Int. J. Heat Mass Transf. 45 (2002) 2011–2020, https://doi.org/10.1016/S0017-9310(01)00314-3.
[53] S.C. Siw, M.K. Chyu, T.I.P. Shih, M.A. Alvin, Effects of pin detached space on heat transfer and pin-fin arrays, J. Heat Transfer. 134 (2012) 1–9, https://doi.org/10.1115/1.4006166.
[54] P.M. Ligrani, M.M. Oliveira, T. Blaskovich, Comparison of heat transfer augmentation techniques, AIAA J. 41 (2003) 337–362, https://doi.org/10.2514/2.1964.
[55] E.M. Sparrow, V.B. Grannis, Pressure drop characteristics of heat exchangers consisting of arrays of diamond-shaped pin fins, Int. J. Heat Mass Transf. 34 (1991) 589–600, https://doi.org/10.1016/0017-9310(91)90108-Q.